Zoosymposia 15: 212–228 (2019)
http://www.mapress.com/j/zs/

ISSN 1178-9905 (print edition)
ZOOSYMPOSIA
ISSN 1178-9913 (online edition)

http://dx.doi.org/10.11646/zoosymposia.15.1.22
http://zoobank.org/urn:lsid:zoobank.org:pub:BA5096F0-B5C6-4900-B2ED-2033F1CC8E5D

Experimental hybridization of sympatric temnopleurid sea urchins living in Yamaguchi, Japan

AKIRA YAMANAKA[1,2,*], YUKI TAKUWA[3] & CHISATO KITAZAWA[3,4]

[1]*Department of Biology & Chemistry, Faculty of Science, Yamaguchi University, Yoshida 1677-1, Yamaguchi 753-8512, Japan*
[2]*Department of Biology, Graduate School of Science and Technology for Innovation, Yamaguchi University, Yoshida 1677-1, Yamaguchi 753-8512, Japan*
[3]*Biological Institute, Faculty of Education, Yamaguchi University, Yoshida 1677-1, Yamaguchi 753-8513, Japan*
[4]*Social System Analysis, The Graduate School of East Asian Studies, Yamaguchi University, Yoshida 1677-1, Yamaguchi 753-8514, Japan*
[*]*Corresponding author, E-mail: yamanaka@yamaguchi-u.ac.jp*

Abstract

Three sympatric species of temnopleurid sea urchins, *Temopleurus toreumaticus* (Leske, 1778), *T. hardwickii* (Gray, 1855) and *Mespilia globulus* (Linnaeus, 1758), occupy a habitat located a short distance from the shore of the Seto Inland Sea, Yamaguchi Prefecture, Japan. Breeding seasons overlap considerably among these species. These species exhibit species-specific differences in embryonic and larval development such as a wrinkled zygote, wrinkled blastula, archenteron invagination, larval skeleton and juvenile morphology. In this study, we determined whether interbreeding among these species is possible. Investigations revealed that fertilization succeeded with all mating combination patterns and that all fertilized eggs developed to the gastrula stage. The blastula and gastrula of hybrids formed in a manner similar to the maternal whereas the developmental delay observed followed the pattern of the paternal species *T. toreumaticus* fertilized at a greater proportion than other pairs and metamorphosed. These results suggest that eggs of this species may have weaker fertilization block in general. At the early developmental stages, hybrid embryos from *T. toreumaticus* mothers express maternal, while some hybrids derived from sperm of *T. toreumaticus* and the eggs of other species ceased development at the 4-armed larval stage. The hybrids of *T. hardwickii* and *M. globulus* ceased development at the gastrula stage, suggesting that these species have a greater degree of genetically isolation distance. In hybrids of *T. toreumaticus* and strongylocentrotid *Hemicentrotus pulcherrimus* (A. Agassiz, 1864), larval skeletons expressed features from both species. These results suggest that traits of hybrids are derived not only from one or both original species, but that a mosaic effect can be obtained depending on the traits. These results indicate that temnopleurids have the weaker fertilization block mechanisms. Isozyme analyses showed that hybrid prisms of *T. toreumaticus* eggs and *M. globulus* sperm possess enzymatic patterns of malate dehydrogenase derived from each parent, whereas the enzymatic pattern of glucose-6-phosphate dehydrogenase is derived from eggs, suggesting that malate dehydrogenase activity may be useful in detecting naturally occurring adult hybrids among these species in the Yamaguchi coastal area.

Key words: Hybridization, temnopleurid sea urchins, malate dehydrogenase, fertilization, development

Introduction

The classification of organisms is based on morphological and genetic traits and genetic isolation according to the biological species concept proposed by Mayr (1969). In this concept, a species is a natural group where individuals can successfully interbreed and be isolated from other groups in term of reproduction.

 Accepted by K. Kanazawa: 6 May 2019; published: 21 Oct. 2019

Reproductive isolation is achieved by a number of specific mechanisms that occur during gamete recognition, fertilization and development (Futuyma 1998).

In an effort to delineate and clarify the mechanisms associated with these barriers, hybrid experiments between species have been studied in many organisms, including sea urchins that have a long history in hybridization experiments (Köhler 1882; Boveri 1889). In sea urchins, although the success of fertilization between different species is restricted in a species-specific manner, or is dependent on the features of the egg or sperm, hybrids sometimes develop depending on the species as described below. In hybrids of a strongylocentrotid *Strongylocentrotus purpuratus* (Stimpson, 1857) and a toxopneusteid *Lytechinus pictus* (Verrill, 1867), expression of ectoderm-specific genes and formation of the larval skeleton is derived from *S. purpuratus* regardless of which species was the mother; it was therefore considered that the traits of hybrids are expressed in a species-specific manner (Brandhorst & Davenport 2001). In hybrids of toxopneusteids *Toxopneustes variegatus* (Lamarck, 1816) and *Hippnoë esculenta* (A. Agassiz, 1872), eggs fertilized in regular sea water or alkaline sea water developed to larvae with skeletons resembling *H. esculenta* in both directions of the cross, while eggs fertilized in acid sea water developed into larvae with skeletons resembling *T. variegatus* (Tennent 1910). In other hand, Onoda (1938) formed hybrids between 10 different species representing 2 orders, 6 families and 10 genera and indicated that in hybrid skeletogenesis the maternal influence is generally stronger than the paternal one. It was also reported that the thermotolerance depends on the egg cytoplasm in hybrids of a dendrasterid *Dendraster excentricus* (Eschscholtz, 1831) and *S. purpuratus* (Fujisawa 1993). Additionally, tropical echinometrids, *Echinometra mathaei* (Blainville, 1825) and *E. oblonga* (Blainville, 1825) or *E.* sp. C can hybridize and develop to mature adults with maternal color pattern and intermediate features including test size, weight, spine length, growth, tube foot and gonad spicule morphology, pedicellaria valve length and gamete size (Rahman & Uehara 2004; Rahman *et al.* 2004). For the hybrids between different developmental types, it is known that echinometrids *Heliocidaris erythogramma* (Valenciennes, 1846), a direct-developing species without food during the larval stage, and *H. tuberculata* (Lamarck, 1816), an indirect developing-species with feeding larval stages, share habitat and breeding season. Eggs of *H. erythogramma* were successfully fertilized by the sperm of *H. tuberculata*, and hybrids developed to larvae with mouths and then metamorphosed into juveniles (Raff *et al.* 1999). The hybrid larvae were similar to dipleurula-type larvae with recent and ancient ancestral features (Raff *et al.* 1999), and ectodermal gene expression patterns (Nielsen *et al.* 2000). Therefore, trait expression in hybrids is dependent, for example, on species, direction of the cross, and rearing conditions.

The development of some temnopleurids has been reported (Mortensen 1921; Fukushi 1959; Okazaki 1975). In *Temnopleurus toreumaticus*, wrinkles form on the surface of fertilized eggs prior to the first cleavage, and wrinkles also form at the blastula stage. These features are absent in *T. hardwickii*, *T. reevesii* (Gray, 1855) and *Mespilia globulus* (Kitazawa *et al.* 2009, 2010) (Fig. 1A–C). Furthermore, it is known that blastulae of *T. toreumaticus* acquire mass ingression of primary mesenchyme cells and that the internal blastular wall acquires species-specific extracellular matrix (Kitazawa *et al.* 2016). At gastrulation, embryos invaginate the archenteron continuously in *T. toreumaticus* or stepwise in the other three species (Takata & Kominami 2004; Kitazawa *et al.* 2016). Following gastrulation, these embryos form primary pore canals from both coelomic pouches to the ectoderm, with movement of these canals differing among species. Subsequently, the right canal disappears (Hara *et al.* 2003; Kitazawa *et al.* 2012, 2014). Their larvae form a cell mass (CM) from the left larval ectoderm at the 2–4-armed larval stage in lieu of the amniotic cavity for adult rudiment formation as seen in every other group of non-cidaroid urchins (Fukushi 1959, 1960; Kitazawa *et al.* 2012, 2014). Although these four species have been considered to be very close species (Matsuoka & Inamori 1996), there are clear differences in their development (Kitazawa *et al.* 2010).

Our previous studies reported that the four species of temnopleurids mentioned above, *T. toreumaticus*, *T. hardwickii*, *T. reevesii* and *M. globulus*, share the same coastal habitat and their breeding seasons are very similar in the Seto Inland Sea, Yamaguchi Prefecture, Japan (Kitazawa *et al.* 2007, 2012, 2014). Interestingly, certain individuals within these populations are sometimes difficult to classify by morphology. In a previous hybrid analysis of temnopleurids, when eggs of *T. toreumaticus* were fertilized with sperm of *M. globulus*, specimens developed into larvae that visually resembled *M. globulus*, while eggs of *M. globulus* that were fertilized with sperms of *T. toreumaticus* developed to larvae with some varieties depending on the year of the experiments (Onoda 1938). However, the detailed larval features of hybrids were not described in that report.

Although the possibility of a sub-species between *T. toreumaticus* and *T. hardwickii* was considered, Matsuoka (1984) indicated that they are very close but different species based on isozyme analysis. A

phylogenetic analysis of *T. toreumaticus*, *T. hardwickii*, *T. reevesii* and *M. globulus* using isozyme analysis indicated that *M. globulus* diverged from an ancestor group ca. 4.5 Mya, *T. hardwickii* at ca. 4 Mya and then *T. toreumaticus* and *T. reevesii* diverged at ca. 2.5 Mya (Matsuoka & Inamori 1996).

In this study we investigated the possibility of interspecies hybrids among temnopleurids, *T. toreumaticus*, *T. hardwickii* and *M. globulus* and the strongylocentrotid *Hemicentrotus pulcherrimus*. We also considered the relationship among species based on a morphological and biochemical analysis of hybrids.

Materials and Methods

Culture

Adult sea urchins of *T. toreumaticus*, *T. hardwickii*, *M. globulus* and *H. pulcherrimus* were collected from the Seto Inland Sea, Yamaguchi Prefecture, Japan. Spawning period was from July to February for *T. toreumaticus*, May to October for *T. hardwickii*, September to February for *M. globulus*, and December to February for *H. pulcherrimus*. Spawning was induced by injecting a small amount of 0.5 M KCl solution into the body cavity. Fertilization and larval cultures were performed according to methods described by Kitazawa *et al.* (2012). The embryos and larvae were cultured at 24°C for temnopleurids species and 18°C for *H. pulcherrimus*. The sperm dilutions and egg concentrations were controlled to the approximately 70% fertilization success in intraspecific controls (egg concentrations were approximately 10^4 eggs/ml; approximately 5×10^{-6} of dry sperm for intraspecific fertilization, approximately 5×10^{-4} for interspecific fertilization). After metamorphosis, the juveniles were cultured in a plastic dish filled with seawater and a piece of seashell coated with algae for food and according to Kitazawa *et al.* (2014).

Hybrid combinations among three temnopleurid species were made by fertilization with eggs (♀) and sperm (♂) derived from another species. The hybrids were derived from eggs of temnopleurid species at 24°C or eggs of *H. pulcherrimus* at 18°C.

Measurement of the archenteron

For calculation of the invagination ratio of the archenteron, the lateral view of embryos at 12–18 h post-fertilization was digitally photographed every hour under a microscope (CX-41, Olympus, Tokyo, Japan) using a digital camera (DP-72, Olympus) and the length of the archenteron and the whole length were measured from the digital images (as shown that invagination of the archenteron starts during 11 h or 14 h post-fertilization for *T. toreumaticus* or *M. globulus*, respectively and that it is difficult to confirm the early invagination because primary mesenchyme cells ingress *en masse* in *T. toreumaticus* (Kitazawa *et al.* 2016), we used embryos after 12 h post-fertilization).

Scanning electron microscopy (SEM) of larval skeleton

Four-armed larvae were transferred to a plastic dish filled with distilled water (DW) for fixing and then transferred onto another dish filled with sea water for several days at 24°C or 10% KOH solution for digestion of organic matter. Skeletal samples were rinsed using DW and then placed on an aluminum tab with conductive aluminum double-sided adhesive tape. The sample tabs were coated using an ion sputter coater (E-1010, Hitachi High-Technologies, Tokyo, Japan) and later observed and photographed using a scanning electron microscope (TM-1000S, Hitachi).

Chemicals

Glucose-6-phosphate (G-6-P), β-nicotinamide adenine dinucleotide (β-NAD^+) and β-nicotinamide adenine dinucleotide phosphate (β-$NADP^+$) were obtained from Oriental Yeast Co. Lit. (Tokyo, Japan). 3,3-[3,3-Dimethoxy-(1,1-biphenyl)-4,4-diyl]-bis[2-(4-nitrophenyl)-5-phenyl-2H tetrazolium chloride (Nitro-TB) and 5-methylphenazinium methyl sulfate (PMS) were purchased from Dojindo Laboratories (Kumamoto, Japan), and malic acids (M) were purchased from Kanto Chemical Co. Lit. (Tokyo, Japan). All other chemicals were of analytical grade.

Preparation of crude enzyme solutions from prisms

Fifteen ml of intraspecific embryonic culture solution of *T. toreumaticus* and *M. globulus*, and hybrid embryonic culture solution of *T. toreumaticus* ♀ × *M. globulus* ♂ that had reached prism stage ca. 16–24 h

post-fertilization were, respectively, centrifuged at 1,000 rpm for 2 min at room temperature (RT). After 14 ml, the upper fraction of each embryonic culture solution was discarded, with the remaining 1 ml of the bottom fraction containing prisms gently pipetted for mixing, the density of intraspecific and hybrid prisms was confirmed in 25 µl samples of the culture solution under a microscope: ca. 97 and 77 intraspecific prisms of *T. toreumaticus* and *M. globulus*, respectively, and 74 hybrid (Hybrid 1) and 501 hybrid (Hybrid 2) prisms of *T. toreumaticus* ♀ × *M. globulus* ♂ in 25 µl of each culture solution. After the embryonic culture solution was spun for 30 sec, the supernatant was removed. Each sample of prisms was homogenized in 200 µl of 50 mM Tris-HCl buffer (pH 7.7) using a motorized tissue grinder (Fisher Scientific, USA), and then centrifuged at 15,000 rpm for 10 min at 4°C. The resulting supernatant was used as a crude enzyme solution of normal and hybrid prisms.

Electrophoresis and isozyme analyses

Sample solutions for electrophoresis were prepared containing 80 µl of crude enzyme solution, 100 µl of 40% sucrose solution containing 0.1% bromophenol blue (BPB) and 20 µl of Tris-glycine electrophoresis buffer (25 mM Tris and 192 mM glycine). Native polyacrylamide gel electrophoresis (PAGE) was performed using 7% polyacrylamide slab gels at 4°C by the method of Davis (1964). Aliquots comprising 25 µl of sample solution were loaded for electrophoretic analysis. Following electrophoresis, the gel was washed briefly in DW, and glucose-6-phosphate dehydrogenase (G6PD) and malate dehydrogenase (MD) enzyme activity was detected by incubating the gel with the following staining solutions; G6PD contained 50 mM Tris-HCl buffer (pH 8.0), 8.3 mM G6P, 165 µM β-$NADP^+$, 367 µM Nitro-TB, 131 µM PMS, and 1.5 mM $MgCl_2$. For MD, G6P and β-$NADP^+$ in the staining solution were replaced with 20 mM M and 162 µM β-NAP^+. The gel was soaked in staining solution at 30°C until the dark blue product became visible, and then kept in a refrigerator to stop the enzyme reaction. Gels were placed on a light box containing an 8W fluorescent tube (FUJICOLOR LIGHT BOX, Fujicolor Co., Japan) and photographed using a digital camera (STYLUS XZ-10, Olympus Co., Japan).

Results

Hybrids among three temnopleurids

To compare the morphological features of intraspecific and hybrid individuals of temnopleurids, we re-examined embryonic and larval development of *T. toreumaticus*, *T. hardwickii* and *M. globulus* (Fig. 1, Tables 1, 2). We confirmed their developmental features as shown in previous studies (Fukushi 1960; Kitazawa *et al.* 2009, 2010, 2012, 2014, 2016). In intraspecific juveniles, new findings on color patterns of the dorsa and triradiate spines (one of two juvenile spine types; triradiate or quadrate dorsal spines) were observed (Table 1; Fig.1A10, B8, C8).

Developmental time course and aspects of developmental characteristics in intraspecific and hybrid individuals of three temnopleurids are summarized in Tables 1 and 2. Fertilization succeeded for all mating combination patterns (Fig. 2A1, B1, C1, D1, E1 and F1). The mean fertilization ratio of each hybrid was 26.9% in *T. toreumaticus* ♀ × *T. hardwickii* ♂ (3 independent experiments, $n = 509$), 18.7% in *T. toreumaticus* ♀ × *M. globulus* ♂ (6 independent experiments, $n = 1{,}309$), ca. 30% in *T. hardwickii* ♀ × *T. toreumaticus* ♂ (n = ca. 200), 15.9% in *T. hardwickii* ♀ × *M. globulus* ♂ ($n = 359$), 13.6% in *M. globulus* ♀ × *T. toreumaticus* ♂ (4 independent experiments, $n = 1{,}005$) and ca. 10% in *M. globulus* ♀ × *T. hardwickii* ♂ (n = ca. 100).

In *T. toreumaticus* ♀ × *T. hardwickii* ♂, fertilized eggs became rough (Fig. 2A2) or had a wrinkled surface (Fig. 2A3) ca. 30 min post-fertilization, and were then smooth and underwent cleavage 1 h post-fertilization (Fig. 2A4). After initial cleavage divisions, wrinkled blastulae formed 5 h post-fertilization (Fig. 2A5). Following the disappearance of wrinkles, blastulae hatched and commenced gastrulation. Embryos where gastrulation had finished had a thick blastular wall, with many mesenchyme cells (Fig. 2A6). These formed 4-armed larvae 2 days post-fertilization, and 1 day later formed a CM on the left side (Fig. 2A7). Out of approximately 300 specimens, 2 specimens metamorphosed over 60 days post-fertilization (Fig. 2A8) and their survival was confirmed up until ca. 2 months after metamorphosis. One juvenile, 45 days post-metamorphosis was colored buff over the entire dorsal side and had needle-like brown juvenile spines with a buff tip (Fig. 2A9).

TABLE 1. Developmental time course of hybrids among three temnopleurids.

Pair of species (fertilization ratio)	Developmental stages (time post-fertilization)*											
	1st	2nd	3rd	4th	5th	6th	B.	G.	4-arm.	6-arm.	8-arm.	Juv.
T. toreumaticus ♀ × ♂	1.5 h	2 h	2.5 h	3 h	3.5 h	4 h	5 h	15 h	2 d	7 d	15 d	29 d
T. hardwickii ♀ × ♂	0.83 h	1.25 h	-†	-†	4.5 h	5.5 h	6 h	23 h	2 d	14 d	23 d	90 d
M. globulus ♀ × ♂	1 h	1.25 h	1.5 h	1.75 h	2.25 h	3 h	4 h	18 h	2 d	7 d	18 d	36 d
T. toreumaticus ♀ × *T. hardwickii* ♂ (26.9%, *n* = 509)	1 h	-†	-†	-†	-†	-†	5 h	(–24 h)	2 d	-†	-†	45d
T. toreumaticus ♀ × *M. globulus* ♂ (18.7%, *n* = 1309)	1.5 h	2 h	2.5 h	3 h	3.5 h	4 h	5 h	17 h	2 d	-†	15 d	41 d
T. hardwickii ♀ × *T. toreumaticus* ♂ (ca. 30%, *n* = ca. 200)	1 h	-†	-†	2.5 h	-†	-†	6 h	24 h	2 d	29 d	dead	
T. hardwickii ♀ × *M. globulus* ♂ (15.9%, *n* = 359)	1 h	2 h	-†	3 h	-†	-†	(–23 h)	dead				
M. globulus ♀ × *T. toreumaticus* ♂ (13.6%, *n* = 1005)	1.5 h	1.75 h	2 h	2.5 h	2.75 h	3.5 h	4 h	19 h	2 d dead			
M. globulus ♀ × *T. hardwickii* ♂ (ca. 10%, *n* = ca. 200)	0.67 h	1 h	1.5 h	-†	-†	-†	-†	24 h dead				

*1st, 2nd, 3rd, 4th, 5th and 6th mean each cleavage. B. and G. mean blastula and gastrula stages. 4-arm., 6-arm. and 8-arm. mean each armed larval stage. Juv. means juvenile stage. “h” and “d” mean hour and days post-fertilization. †Not identified.

TABLE 2. Developmental features of hybrids among three temnopleurids.

Pair of species	Morphology of wrinkled zygotes	Wrinkled blastula	Type of archenteron invagination	Features of juveniles	
				Color of dorsal side	Spines
T. toreumaticus ♀ × ♂	Small uneven* Big fold	Yes**	Continuous***	Olive with 5 radial black pattern	Triradiate, olive with dark brown stripes
T. hardwickii ♀ × ♂	Small uneven Big fold*	Non**	Stepwise***	Buff with Halfmoon black part	Triradiate, buff, brown at the base
M. globulus ♀ × ♂	Small uneven*	Non**	Stepwise***	Red to auburn	Triradiate, short, pointless, red
T. toreumaticus ♀ × *T. hardwickii* ♂	Small uneven Big fold	Yes	-†	Buff with Halfmoon black part	Triradiate, brown, buff at the tip
T. toreumaticus ♀ × *M. globulus* ♂	Small uneven Big fold	Yes	Continuous	-†	Only quadrate dorsal spines
T. hardwickii ♀ × *T. toreumaticus* ♂	Small uneven	Non	-†	-	-
T. hardwickii ♀ × *M. globulus* ♂	Small uneven Big fold	Non	-†	-	-
M. globulus ♀ × *T. toreumaticus* ♂	Small uneven Big fold	Non	Stepwise	-	-
M. globulus ♀ × *T. hardwickii* ♂	Small uneven	Non	-†	-	-

*Kitazawa *et al*. (2010), **Kitazawa *et al.* (2009, 2010), ***Kitazawa *et al*. (2016), Takata & Kominami (2004). †Not identified.

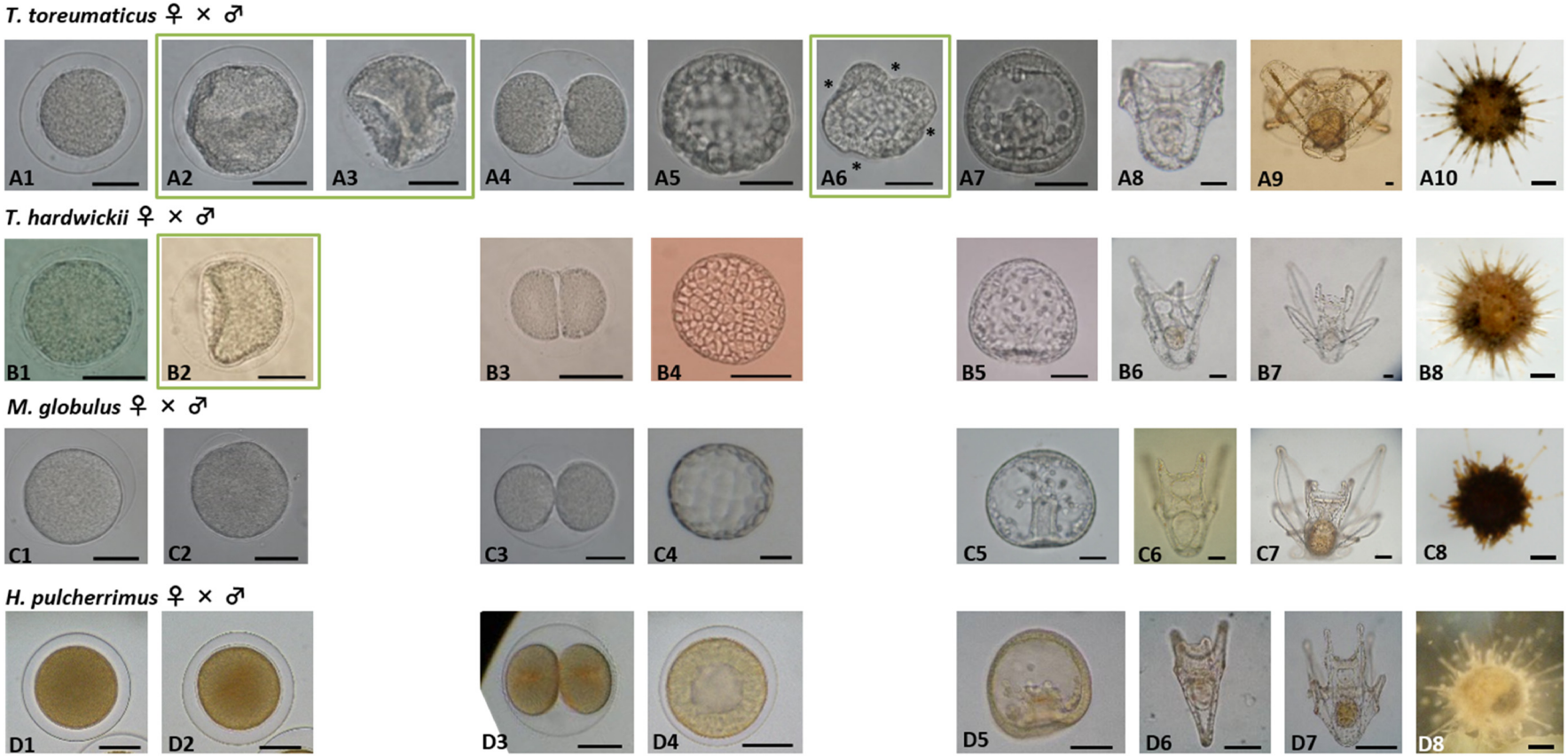

FIGURE 1. Development of sea urchins. A. In *T. toreumaticus*, after fertilization, the zygotes formed wrinkles, became smooth, and then commenced cleavage. The embryos formed wrinkled blastulae. B. In *T. hardwickii*, although a few zygotes formed wrinkles, they never formed wrinkled blastulae. C. *M. globulus* never formed big wrinkles on zygote surfaces or wrinkled blastulae. All of these temnopleurid species formed a cell mass for adult rudiment formation at the early larval stage and metamorphosed after sufficient. Green boxes show wrinkled eggs and blastulae. D. *H. pulcherrimus* also keep smooth zygote surface and formed smooth blastulae with thick blastular wall. This species formed an amniotic cavity for adult rudiment formation at the later larval stage and metamorphosed. * shows a wrinkle. Scale bars = 50 μm for A1−9, B1−7, C1−7 and D1−7, 1 mm for A10 and B−D8.

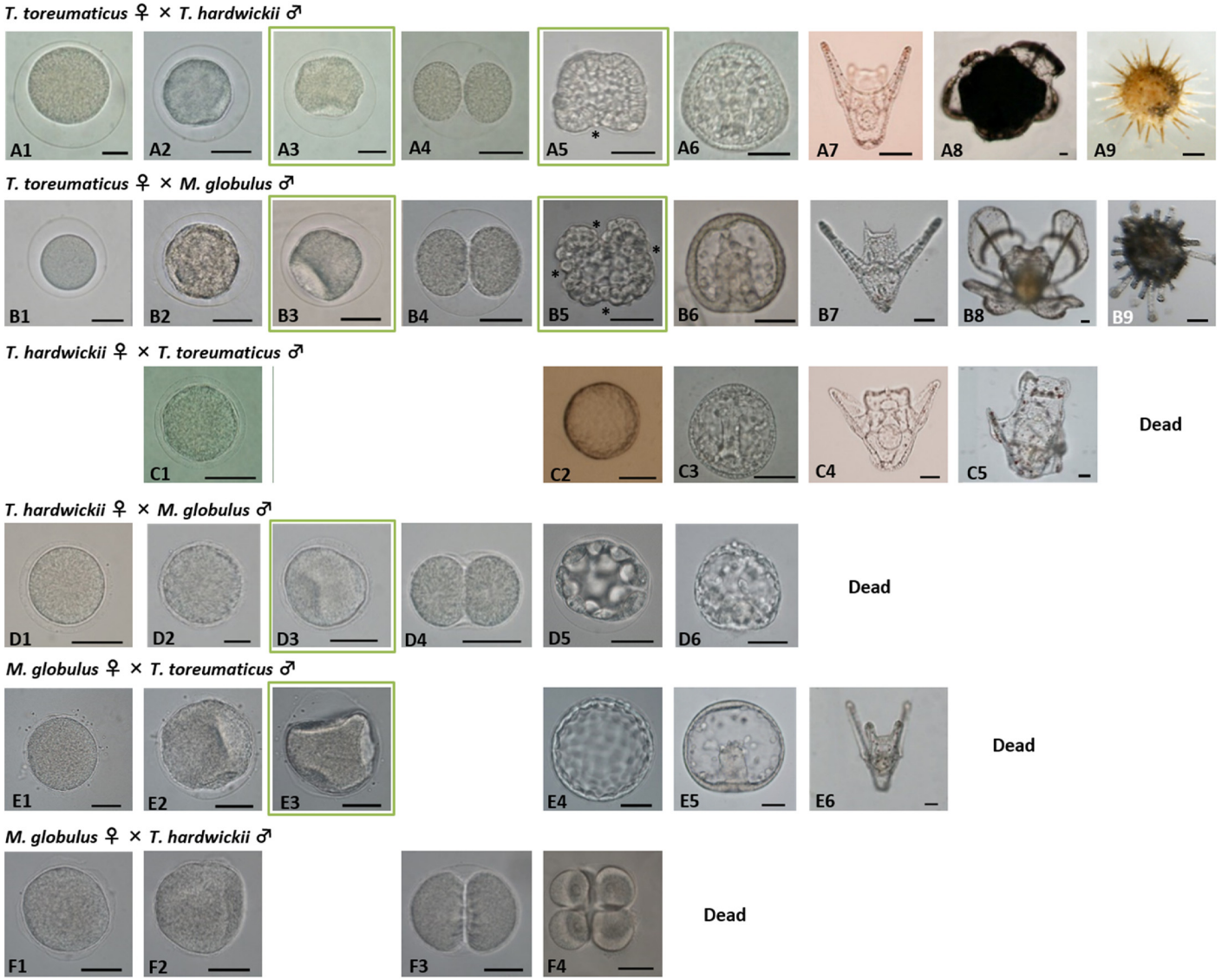

FIGURE 2. Morphology of hybrids. A. *T. toreumaticus* ♀ × *T. hardwikii* ♂. B. *T. toreumaticus* ♀ × *M. globulus* ♂. C. *T. hardwickii* ♀ × *T. toreumaticus* ♂. D. *T. hardwikii* ♀×*M. globulus* ♂. E. *M. globulus* ♀ × *T. toreumaticus* ♂. F. *M. globulus* ♀ × *T. hardwikii* ♂. Green boxes show wrinkled zygotes and blastulae. The * shows a wrinkle. Scale bars = 50 μm for A1−8, B1−8, C1−5, D1−6, E1−6 and F1−4, 1 mm for A9, B9.

In the *T. toreumaticus* ♀ × *M. globulus* ♂ hybrid, 58% of specimens formed a rough (81.5%) (Fig. 2B2) or wrinkled (18.5%) surface (Fig. 2B3) approximately 30 min post-fertilization, while the remainder maintained a smooth surface (n = 58). After the zygote surface became smooth, hybrids underwent cleavage at ca. 30 min to 1.5 h post-fertilization (Fig. 2B4) and formed blastulae by 5 h. Wrinkled blastulae of this hybrid formed in ca. 30 min (Fig. 2B5) as well as those of *T. toreumaticus* (Fig. 1A6). Hybrids slowly developed at the gastrula stage after they became smooth again (Fig. 2B6) and hatched 8.5 h post-fertilization. The invagination ratio of archenteron was calculated as shown in Fig. 3A. Hybrids gastrulated continuously (Fig. 3B, opened squares). The speed of gastrulation was slower than that of intraspecific *T. toreumaticus* (Fig. 3B, closed squares) and faster than that of intraspecific *M. globulus* (Fig. 3B, closed triangles). The hybrids developed to 4-armed larvae at 3 days post-fertilization (Fig. 2B7). Only four specimens of approximately 900 larvae developed to the 6-armed larval stage (Fig. 2B8). Two of these specimens metamorphosed and the juveniles possessed only quadrate dorsal spines (Fig. 2B9).

In *T. hardwickii* ♀ × *T. toreumaticus* ♂, the zygote surface became rough at ca. 50 min post-fertilization (Fig. 2C1) and then became smooth. The hybrids commenced cleavage from 1 h post-fertilization and reached the blastula stage at 6 h (Fig. 2C2), although they did not form wrinkled blastulae. After hatching, gastrulation commenced (Fig. 2C3) and was completed by 24 h post-fertilization. Two-armed larvae with a CM were then formed (Fig. 2C4). Only one out of approximately 100 specimens developed into a 6-armed larva with an abnormal larval skeleton and then died (Fig. 2C5).

In *T. hardwickii* ♀ × *M. globulus* ♂, the zygote surface became rough (Fig. 2D2) or wrinkled (Fig. 2D3) ca. 30 min post-ffertilization and then became smooth forming 2-cell staged embryos 1 h post-fertilization (Fig. 2D4). After cleavages (Fig. 2D5), these formed blastulae with a smooth blastular wall (Table 2). At ca. 23 h post-fertilization, primary mesenchyme cells (PMCs) ingressed and the archenteron invaginated in ≤ 30% of the specimens (Fig. 2D6).

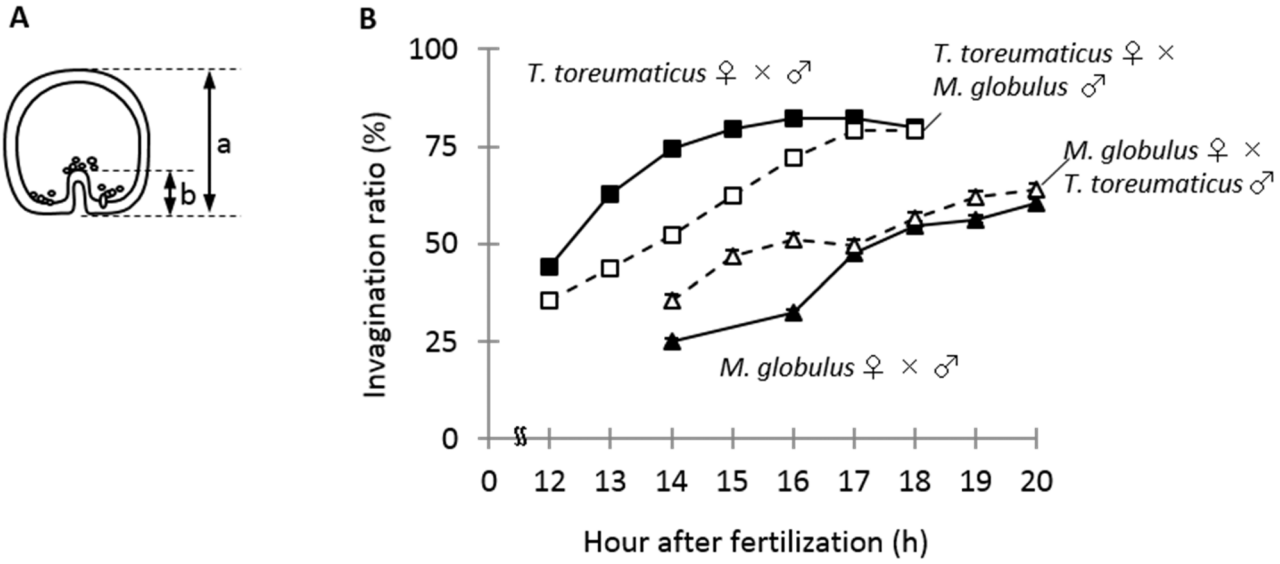

FIGURE 3. Archenteron invagination of hybrids. A. A schematic diagram of the mid-gastrula. As a measure of the invagination ratio of archenteron, we measured the total length of the embryo (a) and the length between the blastopore and the tip of the archenteron wall (b) and then calculated b/a×100 (%). B. Comparison of the rate of archenteron invagination. *T. toreumaticus* (■), *M. globulus* (▲), *T. toreumaticus* ♀ × *M. globulus* ♂ (□) and *M. globulus* ♀ × *T. toreumaticus* ♂ (△). Black lines or black broken lines show original species and hybrids, respectively. Data show mean of 4–38 specimens (bars show SE).

In *M. globulus* ♀ × *T. toreumaticus* ♂, the zygote surface became rough (Fig. 2E2) or wrinkled (Fig. 2E3) ca. 45 min post-fertilization. These underwent cleavage every 15–30 min from 1.5 h post-fertilization and then formed smooth blastulae 4 h after fertilization (Fig. 2E4). Nine hours were needed for hatching, whereas normal *M. globulus* need about 7.5 h. In terms of the ratio of archenteron invagination, the hybrids (Figs. 2E5, 3B, opened triangles) did not elongate the archenteron during 16–17 h post-fertilization, and elongation of the archenteron adopted a stepwise pattern as with normal *M. globulus* (Fig. 3B, closed triangles). The first

invagination of the hybrids began more quickly at the later stage than that of intraspecific *M. globulus,* and the second invagination and completion of gastrulation were delayed slightly. They formed larval skeleton and then at 2 days post-fertilization, hybrids developed into 4-armed larvae (Fig. 2E6) but did not develop further (ca. 700 specimens).

In *M. globulus* ♀ × *T. hardwickii* ♂, hybrid zygote surface became rough ca. 20 min post-fertilization (Fig. 2F2) and then smooth again after cleavage from 40 min post-fertilization (Fig. 2F3). Hybrids developed at the 4-cell stage 1 h post-fertilization and the 8-cell stage 90 min after fertilization (Fig. 2F4). Hybrids formed smooth blastulae and then stopped to develop at the early gastrula stage (ca. 24 h post-fertilization).

SEM observations of larval skeleton in intraspecific and hybrid larvae

Figure 4 shows SEM images of the fenestrated post-oral rods, branched body rods and recurrent rods of intraspecific and hybrid larvae. In intraspecific *T. toreumaticus*, the larvae formed fenestrated post-oral rods with some spines, recurrent and antero-lateral rods with shorter spines and highly branched, curved body rods with spines (Fig. 4A–C). In intraspecific *T. hardwickii*, larvae acquire fenestrated post-oral rods and spines with a narrower angle than larvae of the other two species, which possess recurrent and antero-lateral rods with a few small spines and branched body rods with a few long slender spines (Fig. 4D–F). In intraspecific *M. globulus*, the larval skeleton formed with slightly wide fenestrated post-oral rods and some spines, recurrent, antero-lateral and body rods with spines and body rods with spines that were thick at the base with branches and processes on lines (Fig. 4G–I).

In *T. toreumaticus* ♀ × *M. globulus* ♂ and *M. globulus* ♀ × *T. toreumaticus* ♂, hybrid larvae formed fenestrated post-oral rods, recurrent rods and branches of body rods (Fig. 4J–O). The larvae of *T. toreumaticus* ♀ × *M. globulus* ♂ formed post-oral rods with some slightly slender spines and some processes at equal intervals. The body rods and branches had spines as indicated above. The larvae of *M. globulus* ♀ × *T. toreumaticus* ♂ had wide fenestrated post-oral rods, body rods and recurrent rods, and all of these rods were formed with short thin spines. At the base of the branches of the body rods, a much longer thinner spine with some short processes was present compared to other skeletons.

In an effort to compare the difference in larval skeletons among intraspecific and hybrid larvae, the number of spines/100 μm at post-oral and body rods and the branch of the body rods was counted and the ratio of the length of post-oral rods/the body rods was calculated (Table 3).

The average number of spines of each hybrid larva was more than that of intraspecific larva for each part, although not to greatly. The ratio of the length of post-oral rods/the body rods of each hybrid was intermediate between intraspecific *T. toreumaticus* and *M. globulus* larvae. Overall, it was difficult to determine which traits of the larval skeleton are derived from the egg and the sperm.

TABLE 3. Comparison of spine numbers of larval skeletons in hybrids.

Pair of species	Ratio of length for post-oral rods / Body rods*	Average number of spines/100 μm of each part**		
		Post-oral rods	Body rods	Branch part***
T. toreumaticus ♀ × ♂	2.0 ± 0.1 (27)	0.5 ± 0.0 (13)	0.9 ± 0.1 (14)	2.0 ± 0.1 (19)
T. toreumaticus ♀ × *M. globulus* ♂	1.8 ± 0.1 (16)	0.7 ± 0.1 (12)	0.8 ± 0.0 (11)	2.4 ± 0.2 (11)
M. globulus ♀ × *T. toreumaticus* ♂	1.8 ± 0.2 (9)	0.5 ± 0.1 (17)	1.3 ± 0.2 (15)	2.4 ± 0.2 (13)
M. globulus ♀ × ♂	1.7 ± 0.0 (4)	0.6 ± 0.1 (4)	1.0 ± 0.1 (14)	1.7 ± 0.1 (23)
T. hardwikii ♀ × ♂	1.9 ± 0.4 (4)	0.4 ± 0.1 (4)	0.6 ± 0.1 (3)	1.7 ± 0.3 (4)

The numbers mean data ± SE. The numbers in parentheses indicate specimens including skeletons derived from one side and both sides. *The length of body rods was measured from the base of post-oral rods to the branches at the base. **Each skeleton length was measured, the number of spines counted, and the number of spines per 100 μm of skeleton calculated. ***At the branch part of body rods, the number of spines at both sides from the branch to the tip was counted.

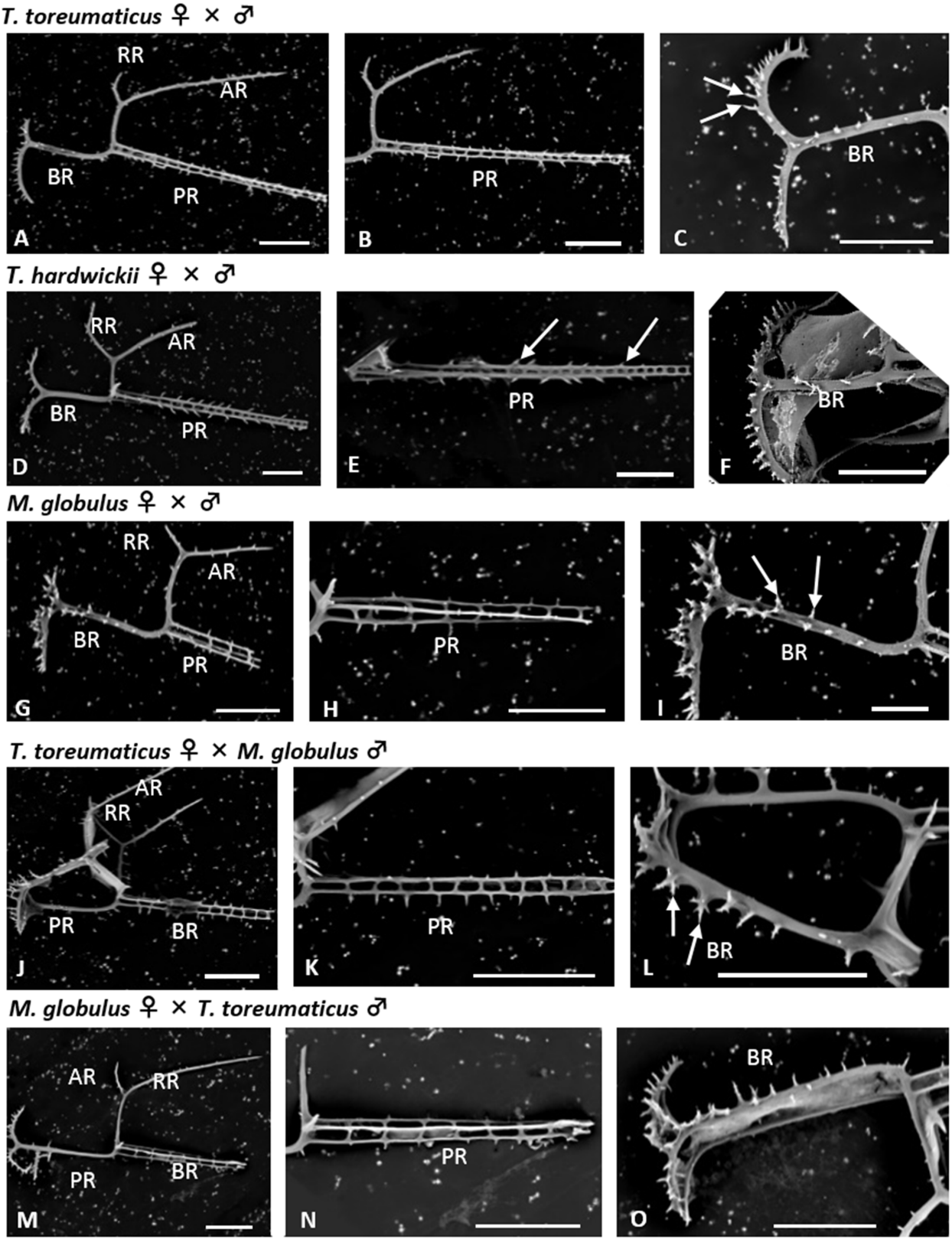

FIGURE 4. Scanning microscopy of larval skeleton at the 4-armed larval stage 3–5 days post-fertilization. A–C. A half skeleton of a larva of *T. toreumaticus*. (B and C) are higher magnifications of post-oral and body rods of (A). D–F. A half skeleton of a larva of *T. hardwickii*. (E) is a higher magnification of the post-oral rod of (D). G–I. A half skeleton of a larva of *M. globulus*. J–L. A skeleton of a larva of *T. toreumaticus* ♀ × *M. globulus* ♂. M–O. A half skeleton of a larva of *M. globulus* ♀ × *T. toreumaticus* ♂. Arrows: spines. AR; antero-lateral rod, BR; body rod, PR; post-oral rod, RR; recurrent rod. Scale bars = 50 μm.

Hybrids of temnopleurids and H. pulcherrimus

Fertilized eggs, embryos and larvae of *H. pulcherrimus*, a strongylocentrotid, exhibited some differences in developmental features to temnopleurids, including smooth fertilized eggs, smooth blastulae, and the formation of an amniotic cavity that is an invagination of the left ectoderm, and that will later form the adult (juvenile) rudiment at the 6-armed larval stage (Figs. 1D1–8, 5A, Table 4).

TABLE 4. Developmental time course of hybrids between *H. pulcherrimus* and temnopleurids.

Pair of species (fertilization ratio)	Developmental stages (time post-fertilization)*			
	Blastula	Gastrula	4-armed larva	6-armed larva
H. pulcherrimus ♀ × *T. toreumaticus* ♂ (10.9%, *n* = 109)	7 h	-†	3 d	6 d dead
T. toreumaticus ♀ × *H. pulcherrimus* ♂ (26.9%, *n* = 509)	6.5 h	-†	2 d dead	
M. globulus ♀ × *H. pulcherrimus* ♂ (7.3%, *n* = 245)	-†	(–2 d) dead		

* "h" and "d" mean hour and days post-fertilization. †Not identified.

The fertilization ratio was 10.9 % in *H. pulcherrimus* ♀ × *T. toreumaticus* ♂ crosses (*n* = 109). After the fertilized eggs cleaved, this hybrid formed blastulae with a smooth blastular wall ca. 7 h post-fertilization at hatching. After gastrulation, hybrids developed to prism larvae by 2 days post-fertilization, and 4-armed larvae by 3 days. One out of 50 specimens developed into a 6-armed larva with an amniotic cavity by 6 days (Fig. 5B), but did not survive further.

In *T. toreumaticus* ♀ × *H. pulcherrimus* ♂, the fertilization ratio was 6.3% (*n* = 176). Approximately 30 min post-fertilization, the zygote surface became rough or wrinkled and then smooth again. Hybrids underwent cleavage and then formed wrinkled blastulae ca. 6.5 h after fertilization (Fig. 5C). After becoming smooth again, hybrids hatched and started gastrulation. Hybrids formed 4-armed pluteus larvae with a CM at 2 days post-fertilization (Fig. 5D). All of these larvae had short post-oral arms, and failed to survive after 7 days (*n* = 7).

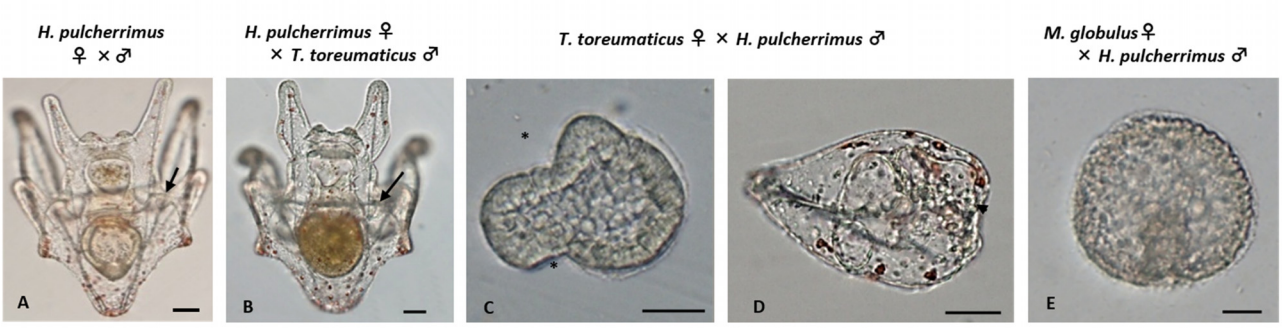

FIGURE 5. Development of hybrids between *H. pulcherrimus* and temnopleurid sea urchins. A. A 6-armed larva (ventral view) of *H. pulcherrimus*. B. A 6-armed larva of *H. pulcherrimus* ♀ × *T. toreumaticus* ♂ with an amniotic cavity (ventral view). C and D. *T. toreumaticus* ♀ × *H. pulcherrimus* ♂. The embryo formed a wrinkled blastula and then developed to a larva with a cell mass. E. A mid-gastrula derived from *M. globulus* ♀ × *H. pulcherrimus* ♂. Arrows; amniotic cavity, arrowhead; cell mass. The * shows a wrinkle. Scale bars = 50 µm.

In *M. globulus* ♀ × *H. pulcherrimus* ♂, the fertilization ratio was 7.3% (*n* = 245). Following early cleavages, they developed to blastulae and started gastrulation, but they failed to develop further at the mid-gastrula stage at 2 days post-fertilization (Fig. 5E). The hybridization of *H. pulcherrimus* ♀ × *M. globulus* ♂ was not made as sperm of *M. globulus* was not obtained.

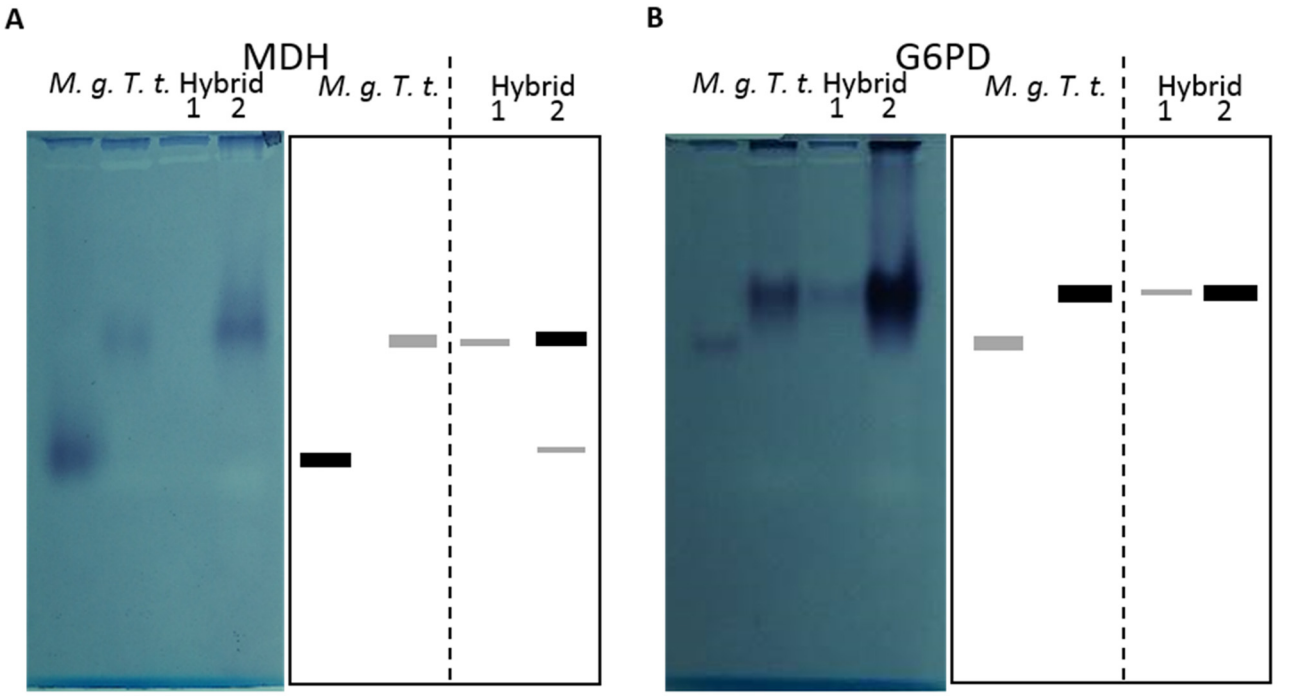

FIGURE 6. Isozyme analysis of sea urchins. Gels and schematic diagrams for MDH (A) and G6PD (B). *M. g.* ; normal prisms of *M. globulus*, *T. t.* ; normal prisms of *T. toreumaticus*, Hybrid 1 and 2; hybrid prisms approximately 24 h after fertilization derived from *T. toreumaticus* ♀ × *M. globulus* ♂.

Isozyme analysis

Figure 6 shows isozyme patterns of MDH and G6PD of normal prisms of *M. globulus*, *T. toreumaticus*, and hybrid prism larvae of *T. toreumaticus* ♀ × *M. globulus*. Each sample of Hybrid 1 and 2 (see Materials and Methods) was prepared from independent culture experiments. Hybrid 2 possessed two bands showing MDH activity derived from each parent, whereas Hybrid 1 possessed one band derived from eggs of *T. toreumaticus* (Fig. 6A). Both Hybrid 1 and 2 possessed one band showing G6PD activity derived from eggs of *T. toreumaticus*, and not derived from sperm of *M. globulus* (Fig. 6B). These results indicate that hybrid prisms did not always possess the isozyme patterns derived from each parent, and suggest that comparison of isozyme patterns of MDH may be useful in identifying hybrids among temnopleurid sea urchins.

Discussion

In the present study, hybridization of three temnopleurid species and between different families, Temnopleuridae and Strongylocentrotidae, resulted in successful fertilization and development to at least the gastrula stage (Tables 1, 2, Figs. 2, 5). Although Onoda (1938) reported that in *H. crassispina* (A. Agassiz, 1864) ♀ × *T. toreumaticus* ♂ or *M. globulus* ♀ × *H. crassispina* ♂, chromosomes were eliminated at the first cleavage for expression of either parent feature, this was not the case with the zygotes in the present study and the embryos possessed similar size of nuclei as in the parents. In part of the hybridization, isozyme analysis showed enzyme activity patterns derived from each parent (Fig. 6A, B) and these results indicate that hybridization succeeded.

Kato & Sugiyama (1978) reported that fertilization does not occur between species in a same family, such as between echinometrids, *E. mathaei* and *H. crassispina* or between strongylocentrotids, *H. pulcherrimus* ♀ and *Pseudocentrotus depressus* (A. Agassiz, 1864) ♂. However, in this study, fertilization between any pair succeeded, and especially in the case of hybridization that involved the eggs of *T. toreumaticus*; this species had 1.2–2.7 fold higher fertilization success than other species. Onoda (1938) also described that the eggs of *T. toreumaticus* seem to be easily hybridized with sperms of other species. However, both hybrids of *T. hardwickii* × *M. globulus* ceased development at the gastrula stage, indicating that genetic isolation certainly exists between these two species. These results suggest that among the three temnopleurid species, eggs of *T.*

toreumaticus acquire the weakest fertilization block mechanisms in relation to, for example, to block fertilization, such as a thick, jelly-like egg surface structure, sperm morphology, and sperm-binding proteins. It is known that divergence of sperm-egg recognition protein bindin may cause gamete incompatibility (Zigler *et al.* 2005, 2012). Onoda (1938) reported that the size of sperm head of *T. toreumaticus* was the smallest among four species including *E. mathaei*, a toxopneustid *T. pileolus* (Lamark, 1816), *H. crassispina* and *T. toreumaticus* (mean approximately 1.7 µm). It is considered that the success of fertilization for the sperms with the small heads needs eggs with less jelly and weak membrane structure. Furthermore, it has been reported that zygotes of *T. toreumaticus* can be wrinkled and form wrinkled blastulae (Kitazawa *et al.* 2009, 2010), suggesting that the flexible structure of the zygote surface of this species may play a role in the weaker fertilization block mechanisms.

In terms of traits observed during development, wrinkled blastula formation was identified in all hybrids involving eggs of *T. toreumaticus*, and archenteron invagination was continuous in *T. toreumaticus* ♀ × *M. globulus* ♂ and stepwise in *M. globulus* ♀ × *T. toreumaticus* ♂ (Table 2). These results suggest that wrinkled blastula formation and the manner by which archenteron invagination occurs (continuous vs. stepwise) are dependent on the eggs. The same maternal trait of wrinkled blastula formation in *H. erhthrogramma* ♀ × *H. tuberculata* ♂ was reported by Raff *et al.* (1999). Also, the hybrid gastrula of *T. toreumaticus* × *M. globulus* formed in a manner relatively similar to the maternal developmental mode (Fig. 3B). On the other hand, the dorsal body color of juveniles may be depending on sperm since the color of the juveniles of *T. toreumaticus* ♀ × *T. hardwickii* ♂ was similar to one of the males (Figs. 1B8, 2A9, Tables 1, 2).

In terms of developmental pace, *T. toreumaticus* ♀ × *M. globulus* ♂ development was delayed after the blastula stage when compared to *T. toreumaticus* ♀ × ♂, while in *M. globulus* ♀ × *T. toreumaticus* ♂ development was delayed at the early cleavages and after the blastula stage when compared to *M. globulus* ♀ × ♂ (Table 1). Furthermore, hybridization of eggs of *T. toreumaticus* caused delays after hatching. On the other hand, other pairs were delayed in development from the cleavage stages and the hybrids ceased to develop at the gastrula stage and larval stages and did not metamorphose (Table 1). Additionally, hybrids derived from eggs of *T. toreumaticus* expressed some maternal traits at the early stage (Fig. 2, Table 2). These results suggest that in *T. toreumaticus*, the embryos develop in the maternal manner at the early stage while later they follow the paternal manner. In the other 2 species, however, embryos express paternal traits from early development. These modes of embryonic development presumably enabled hybrids derived from eggs of *T. toreumaticus* to develop to juveniles, while ones derived from eggs of the other two species and sperm of *T. toreumaticus* ceased development. This means that in each species the timing to express maternal or paternal traits is determined for normal embryonic development. This is supported by the fact that *H. erythogramma* ♀ × *H. tuberculata* ♂ developed to metamorphosis, while *H. tuberculata* ♀ × *H. erythogramma* ♂ ceased development at the gastrula stage (Raff *et al.* 1999).

Our results indicate that isozyme analysis of intraspecific and hybrid prisms is useful when employing 150 to 1,000 specimens / 25 µl sample solution (Fig. 6A, B; lanes *M. g.*, *T. t*. and Hybrid 2). We are unable to account for the very weak MDH activity in Hybrid 1, although the embryonic density of Hybrid 1 was similar to that of intraspecific *M. globulus* in the culture solutions. In this study, only one isozyme of MDH and G6PD was detected in normal prisms of *M. globulus* and *T. toreumaticus* (Fig. 6A, B). Interestingly, Matsuoka (1984) reported three MDH isozymes present in the gonads of adult *T. toreumaticus*. In preliminary experiments, we detected the presence of three bands showing MDH activity in crude extracts prepared from a small amount of gonads of *M. globulus* (data not shown), although normal prisms possessed only one band showing MDH activity (Fig. 6A).

Additional analysis is required using hybrid juveniles or gonads of *T. toreumaticus* ♀ × *M. globulus* ♂ since two hybrids of *T. toreumaticus* ♀ × *M. globulus* ♂ and *T. toreumaticus* ♀ × *T. hardwickii* ♂ develop into adults in our laboratory (Fig. 2A9, B9). Furthermore, a search for natural hybridization in the Seto Island Sea area of Yamaguchi Prefecture is also required.

Some reports indicated that sympatric echinoid species are isolated by prezygotic isolating barriers including differences in microhabitats, breeding seasons (Lessios 2007), environmental conditions like temperature (Fujisawa 1993) and alkalinity (Tennent 1910). On the coasts of Yamaguchi area, we can find the adults of the temnopleurids, and we made field survey over 10 years. At the spring ebb tide, adults of *T. hardwickii* wearing algae appear on the sandy beach. *T. toreumaticus* adults are found in muddy shore mostly during summer, while adults of *M. globulus* hide under stones during summer. Many *H. pulcherrimus* can always be found in rocky shore. Their breeding seasons in Yamaguchi area are from May to October for *T.*

hardwickii (in the present study), from July to October for *T. toreumaticus* (Kitazawa *et al.* 2007, 2014), from July (to around October) for *M. globulus* (Kitazawa *et al.* 2012) and from late December to middle of April for *H. pulcherrimus* (Kitazawa *et al.* 2007). However, in spite of the same breeding season and luna spawning cycle in sympatric habitat, reproduce isolation is caused by slight differences in temperature tolerance for spawning, fertilization and development (Lessios & Pearse 1996; McClary & Swell 2003; Rahman & Uehara 2004; Rahman *et al.* 2004). In many species, therefore, hybrids can be produced only in lab (Lessios & Pearse 1996; Lessios 2007). In the present study, the hybridization in the lab occurred successfully because the breeding seasons of the temnopleurids were overlapped. In our other experiment, embryonic culture of *T. hardwickii* at 24°C sometimes causes to die, and in much colder conditions embryos of *T. hardwickii* survive better than those other temnopleurids. Different temperature tolerance in embryonic development could correlate with different spawning temperature, causing a prezygotic isolating barrier. The hybridization in the nature may occur limited to a short term in particular condition. To analyze their breeding behavior including pheromone use will be helpful to understand the reproductive isolation of these species.

Recently, Lamare *et al.* (2018) reported developmental thermal windows in native and hybrid progeny of txopneustids *Pseudoboletia maculata* (Troschel, 1869) and *P. indiana* (Michelin, 1862), which have overlapping distributions in the Pacific and readily hybridize. Their hybrids were less tolerant of the warmer conditions experienced by the *Pseudoboletia* species, indicating that the fitness of progeny limits distribution of the hybrids. Also, the larval distribution and viability and growth of adults are important for postzygotic isolation (Rahman *et al.* 2000; Harper *et al.* 2007). Future studies will need the hybrid juvenile culture for analyses of gonad development and backcross of hybrids, as well as comparison of the microhabitats of the temnopleurid species and hybrids in Yamaguchi area.

Acknowledgements

We appreciate the Department of Fishery in Yamaguchi Prefecture and Yamaguchi Fisheries Cooperative Association for permission to collect sea urchins.

References

Boveri, T. (1889) Ein geschlechtlich erzeugter organismus ohne mutterliche eigenschaften. *Sitzber Gesellschaft für Morphologie und Physiologie München*, 5, 73–83.

Brandhorst, B.P. & Davenport, R. (2001) Skeletogenesis in sea urchin interordinal hybrid embryos. *Cell and Tissue Research*, 30, 159–167.
https://doi.org/10.1007/s004410100381

Davis, B.J. (1964) Disc electrophoresis II. Method and application to human serum proteins. *Annals of the New York Academy of Science*, 121, 404–427.
https://doi.org/10.1111/j.1749-6632.1964.tb14213.x

Fujisawa, H. (1993) Temperature sensitivity of a hybrid between two species of sea urchin differing in thermotolerance. *Development Growth & Differentiation*, 35 (4), 395–401.
https://doi.org/10.1111/j.1440-169X.1993.00395.x

Fukushi, T. (1959) On the cell mass observed on the left side of the pluteus of the sea urchin, *Temnopleurus hardwickii*. *The bulletin of the Marine Biological Station of Asamushi*, 9, 133–135.

Fukushi, T. (1960) The formation of the echinus rudiment and the development of the larval form in the sea urchin, *Temnopleurus hardwickii*. *The bulletin of the Marine Biological Station of Asamushi*, 10, 65–72.

Futuyma, D.J. (1998) *Evolutionary Biology.* Sinauer Associates, Sunderland, Massachusetts.

Hara, Y., Kuraishi, R., Uemura, I. & Katow, H. (2003) Asymmetric formation and possible function of the primary pore canal in plutei of *Temnopleurus hardwickii*. *Development, Growth & Differentiation*, 45, 295–308.
https://doi.org/10.1046/j.1440-169X.2003.00697.x

Harper, F.M., Addison, J.A. & Hart, M.W. (2007) Introgression versus immigration in hybridizing high-dispersal echinoderms. *Evolution*, 61–10, 2410–2418.
https://doi.org/10.1111/j.1558-5646.2007.00200.x

Kato, K.H. & Sugiyama, M. (1978) Species-specific adhesion of spermatozoa to the surface of fixed eggs in sea urchins. *Development, Growth & Differentiation*, 20, 337–347.

https://doi.org/10.1111/j.1440-169X.1978.00337.x
Kitazawa, C., Kawasaki, S., Nishimura, H., Nakano, M., Yamaguchi, T. & Yamanaka, A. (2007) Distribution and habitat preferences of sea urchin species in Shirikawa Bay, Yamaguchi, during the period from 2005 to 2007. *Bulletin of the Faculty of Education, Yamaguchi University*, 57, 95–105.
Kitazawa, C., Nishimura, H., Yamaguchi, T., Nakano, M. & Yamanaka, A. (2009) Novel morphological traits in the early developmental stages of *Temnopleurus toreumaticus*. *The Biological Bulletin*, 217, 215–221.
https://doi.org/10.1086/BBLv217n3p215
Kitazawa, C., Tsuchihashi, Y., Egusa, Y., Genda, T. & Yamanaka, A. (2010) Morphogenesis during early development in four Temnopleuridae sea urchins. *Information*, 13, 1075–1089.
Kitazawa, C., Kobayashi, C., Kasahara, M., Takuwa, Y. & Yamanaka, A. (2012) Morphogenesis of adult traits during the early development of *Mespilia globulus* Linnaeus, 1758 (Echinodermata: Echinoidea). *Zoological Studies*, 51, 1481–1489.
Kitazawa, C., Sakaguchi, C., Nishimura, H., Kobayashi, C., Baba, T. & Yamanaka, A. (2014) Development of the sea urchin *Temnopleurus toreumaticus* Leske, 1778 and *Temnopleurus reevesii* Gray, 1855 (Camarodonta: Temnopleuridae). *Zoological Studies*, 53, 3.
https://doi.org/10.1186/1810-522X-53-3
Kitazawa, C., Fujii, T., Egusa, Y., Komatsu, M. & Yamanaka, A. (2016) Morphological diversity of blastula formation and gastrulation in temnopleurid sea urchins. *Biology Open*, 5, 1555–1566.
https://doi.org/10.1242/bio.019018
Köhler, M.R. (1882) On some experiments in hybridization between different species of Echinoidea. *Annals and Magazine of Natural History*, 10, 179–180.
https://doi.org/10.1080/00222938209459691
Lamare, M., Harianto, J., Uthicke, S., Agüera, A., Karelitz, S., Pecorino, D., Chin, J. & Byrne, M. (2018) Larval thermal windows in native and hybrid *Pseudoboletia* progeny (Ehinoidea) as potential drivers of the hybridization zone. *Marine Ecology Progress Series*, 598, 99–112.
https://doi.org/10.3354/meps12601
Lessios, H.A. (2007) Reproductive isolation between species of sea urchins. *Bulletin of Marine Science*, 81 (2), 191–208.
Lessios, H.A. & Pearse, J.S. (1996) Hybridization and introgression between Indo-Pacific species of *Diadema*. *Marine Biology*, 126, 715–523.
https://doi.org/10.1007/BF00351338
Matsuoka, N. (1984) Electrophoretic evolution of the taxonomic relationship of two species of the sea-urchin, *Temnopleurus toreumaticus* (LESKE) and *T. hardwickii* (GRAY). *Proceedings of the Japanese Society of Systematic Zoology*, 29, 30–36.
Matsuoka, N. & Inamori, M. (1996) Phylogenetic relationships of echinoids of the family Temnopleuridae inferred from allozyme variation. *Genes & Genetic Systems*, 71, 203–209.
https://doi.org/10.1266/ggs.71.203
Mayr, E. (1969) *Principles of Systematic Zoology*. McGraw-Hill, New York.
Mortensen, T.H. (1921) *Studies of the Development and Larval Forms of Echinoderms.* G. E. C. GAD, Copenhagen.
https://doi.org/10.5962/bhl.title.11376
McClary, D.J. & Swell, M.A. (2003) Hybridization in the sea: gametic and developmental constraints on fertilization in sympatric species of *Pseudechinus* (Echinodermata: Echinoidea). *Journal of Experimental Marine Biology and Ecology*, 284, 51–70.
https://doi.org/10.1016/S0022-0981(02)00487-2
Nielsen, M.G., Wilson, K.A., Raff, E.C. & Raff, R.A. (2000) Novel gene expression patterns in hybrid embryos between species with different modes of development. *Evolution & Development*, 2 (3), 133–144.
https://doi.org/10.1046/j.1525-142x.2000.00040.x
Okazaki, K. (1975) 7. Normal development to metamorphosis. *In*: Czihak, G. (Ed.), *The Sea Urchin Embryo Biochemistry and Morphogenesis*. Springer-Verlag, Berlin, pp. 177–232.
https://doi.org/10.1007/978-3-642-65964-5_9
Onoda, K. (1938) Hybridization experiments in some echinoids. *Japanese Journal of Genetics*, 13, 306–320. [in Japanese]
https://doi.org/10.1266/jjg.13.306
Raff, E.C., Popodi, E.M., Sly, B.J., Turner, F.R., Villinski, J.T. & Raff, R.A. (1999) A novel ontogenetic pathway in hybrid embryos between species with different modes of development. *Development,* 126, 1937–1945.
Rahman, M.A. & Uehara, T. (2004) Interspecific hybridization and backcrosses between two sibling species of pacific sea urchin (Genus *Echinometra*) on Okinawan intertidal reefs. *Zoological Studies*, 43 (1), 93–111.
Rahman, M.A., Uehara, T. & Aslan, L.M. (2000) Comparative viability and growth of hybrids between sympatric species of sea urchins (Genus *Echinometra*) in Okinawa. *Aquaculture*, 183, 45–56.
https://doi.org/10.1016/S0044-8486(99)00283-5

Rahman, M.A., Uehara, T. & Pearse, J.S. (2004) Experimental hybridization between two recently diverged species of tropical sea urchins, *Echinometra mathaei* and *Echinometra oblonga*. *Invertebrate Reproduction and Development*, 45 (1), 1–14. https://doi.org/10.1080/07924259.2004.9652569

Takata, H. & Kominami, T. (2004) Behavior of pigment cells closely correlates the manner of gastrulation in sea urchin embryos. *Zoological Science,* 21, 1025–1035. https://doi.org/10.2108/zsj.21.1025

Tennent, D.H. (1910) The dominance of maternal or of paternal characters in echinoderm hybrids. *Archiv für Entwicklungsmechanik der Organismen*. 29, 1–14. https://doi.org/10.1007/BF02297061

Zigler, K.S, Byrne, M., Raff, E.C., Lessios, H.A. & Raff, R.A. (2012) Natural hybridization in the sea urchin genus *Pseudoboletia* between species without apparent barriers to gamete recognition. *Evolution*, 66–6, 1695–1708. https://doi.org/10.1111/j.1558-5646.2012.01609.x

Zigler, K.S., McCartney, M.A., Levitan, D.R. & Lessios, H.A. (2005) Sea urchin bindin divergence predicts gamete compatibility. *Evolution*, 59 (11), 2399–2404. https://doi.org/10.1554/05-098.1